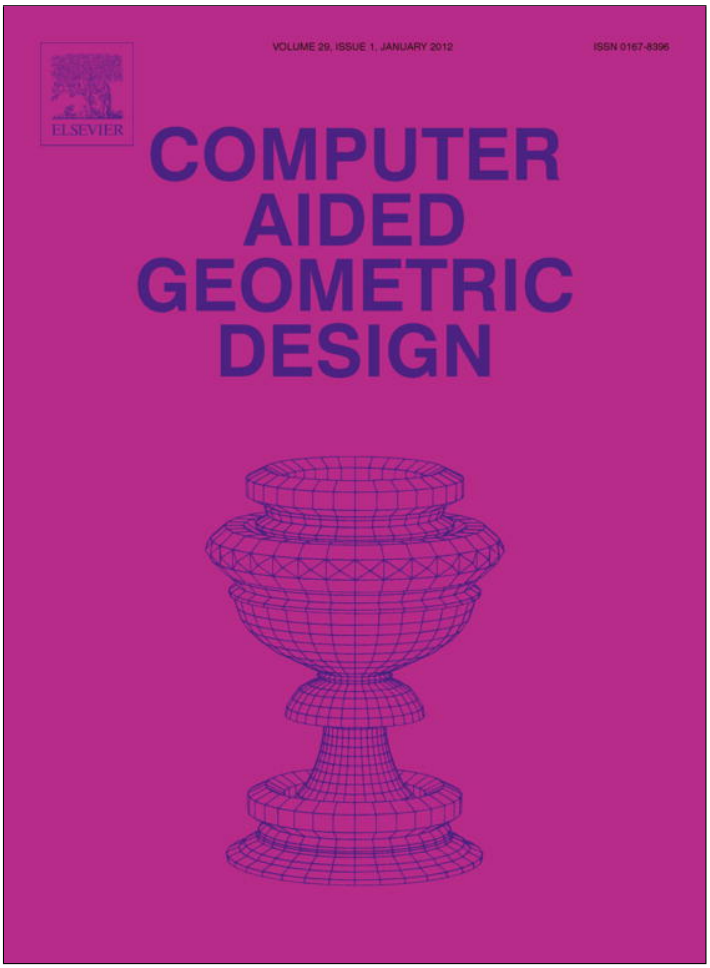

Computer Aided Geometric Design 29 (2012) 63–76

Contents lists available at SciVerse ScienceDirect

Computer Aided Geometric Design

www.elsevier.com/locate/cagd

On linear independence of T-spline blending functions ☆

Xin Li [a], Jianmin Zheng [b], Thomas W. Sederberg [c,*], Thomas J.R. Hughes [d], Michael A. Scott [d]

[a] University of Science and Technology of China, Hefei, Anhui, PR China
[b] School of Computer Engineering, Nanyang Technological University, Singapore
[c] Computer Science Department, Brigham Young University, United States
[d] ICES, University of Texas at Austin, United States

ARTICLE INFO

Article history:
Received 14 October 2010
Received in revised form 23 August 2011
Accepted 29 August 2011
Available online 22 September 2011

Keywords:
T-splines
Blending functions
Linear independence
NURBS
Isogeometric analysis

ABSTRACT

This paper shows that, for any given T-spline, the linear independence of its blending functions can be determined by computing the nullity of the T-spline-to-NURBS transform matrix. The paper analyzes the class of T-splines for which no perpendicular T-node extensions intersect, and shows that the blending functions for any such T-spline are linearly independent.

1. Introduction

T-splines (Sederberg et al., 2003, 2004) are a free-form geometric shape technology that solves many of the limitations inherent in the industry standard NURBS representation.

One advantage that T-splines have over NURBS is local refinement. While NURBS refinement requires the insertion of an entire row of control points, T-splines allow partial rows of control points that terminate in a special control point called a T-junction. Another advantage is that T-spline models are watertight, whereas NURBS models are typically comprised of many distinct patches that do not generally fit together without gaps. In particular, most trimmed NURBS models have mathematically unavoidable gaps which can be completely closed using an extension to T-splines (Sederberg et al., 2008). T-splines are forward and backward compatible with NURBS surfaces, and thus integrate well into existing CAD systems.

These capabilities that make T-splines attractive for use in CAD have also made T-splines desirable for use in isogeometric analysis (Hughes et al., 2005, Cottrell et al., 2009, Bazilevs et al., 2010). Local refinement is valuable in analysis because it enables much smaller linear systems than would a similar NURBS solution. Watertightness is valuable because models that are not watertight often require substantial preprocessing to close the unwanted gaps, and in the process the "isogeometric" principle of using the identical model for CAD and analysis is violated. NURBS compatibility is valuable because NURBS is an industry standard CAD representation and widespread industrial adoption of isogeometric analysis will occur most easily with technologies that are compatible with existing standards.

A property that has not been studied for T-splines until recently is linear independence of blending functions. While linear independence is not required (although desirable) for most CAGD applications, it is imperative for isogeometric analysis.

☆ This paper has been recommended for acceptance by Jörg Peters.

* Corresponding author.
E-mail address: tom@cs.byu.edu (T.W. Sederberg).

0167-8396/$ – see front matter
doi:10.1016/j.cagd.2011.08.005

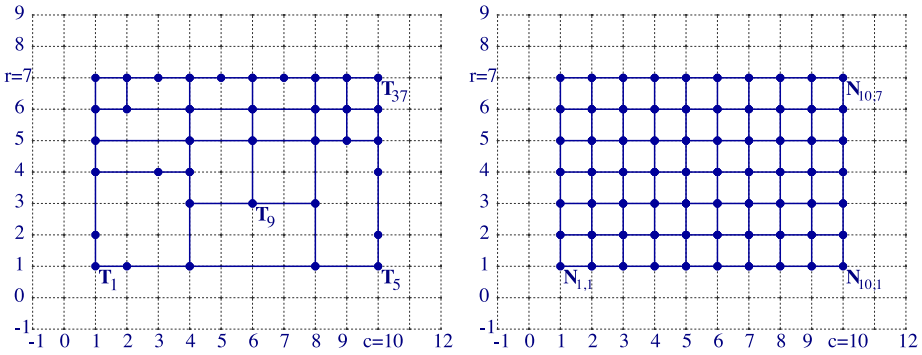

(a) T-mesh. (b) Underlying NURBS.

Fig. 1. Knot index diagrams.

Linear dependencies are never allowed in practice in a finite element basis, since the equation system is not invertible, and squaring the system (as is done in a least squares approach) does not remove rank deficiency. While redundancies can be removed and the reduced squared system formed, this is a risky approach since the condition number is also squared in the process. Consequently, techniques like this were purged from the FEA literature 50 years ago. Thus, the analysis community requires bases that are assured *a priori* to be linearly independent.

Unfortunately, Buffa et al. (2010) give an example of a T-spline with linearly dependent blending functions, raising concerns that T-splines in their full generality may not be suitable for use in isogeometric analysis. Buffa et al. (2010) also present a constructive method for devising a class of T-splines whose blending functions *are* linearly independent. However, it is not obvious how to use the method to check whether a given T-spline control mesh can be constructed using the method. Also, not all T-splines with linearly independent blending functions can be obtained in this manner.

This paper identifies a class of T-splines whose blending functions are guaranteed to be linearly independent. T-splines in this class obey the simple requirement that no two orthogonal T-node extensions (see Section 6) are allowed to intersect. Like all T-splines, members of this class provide watertight models, are NURBS compatible, obey the convex hull property, and are affine invariant—all important properties for isogeometric analysis. Furthermore, algorithms have been devised whereby local refinement of such T-splines is well contained (Scott et al., 2011). Also, under an additional minor condition, the polynomial blending functions for such T-splines sum identically to one (Li et al., 2011). For these reasons, T-splines whose T-node extensions do not intersect are well-suited for isogeometric analysis, and we will refer to them as *analysis-suitable T-splines*.

The paper is structured as follows. Pertinent background on T-splines is reviewed in Section 2. Section 3 discusses how to construct a matrix M that maps T-spline control points to the control points of an equivalent NURBS surface. Section 4 proves that M being full rank is a necessary and sufficient condition for the blending functions of a T-spline to be linearly independent. Section 5 explains how T-mesh topology influences non-zero elements of M. This insight is used in Section 6 to prove that any analysis-suitable T-spline has linearly independent blending functions.

This paper is written specifically in terms of bicubic T-splines, although the concepts should extend to any degree. T-splines of arbitrary degree are discussed in Finnigan (2008), Bazilevs et al. (2010). The dimension of T-spline spaces is analyzed in Mourrain (2010).

2. T-splines

A T-spline is defined in terms of a control grid (or, T-mesh) and global knot vectors $\vec{\mathbf{s}} = [s_{-1}, s_0, s_1, \ldots, s_{c+2}]$ and $\vec{\mathbf{t}} = [t_{-1}, t_0, t_1, \ldots, t_{r+2}]$. Each control point $\mathbf{T}_i$ corresponds to a unique pair of knots (s_j, t_k), and we will refer to (j, k) as the index coordinates of $\mathbf{T}_i$. Fig. 1 illustrates T-spline and NURBS *knot index diagrams*, in which control points are drawn on their respective index coordinates. In a T-mesh, control points occupy some, but not all, $(j, k) \in \mathbb{Z}^2$ within $[1, c] \times [1, r]$, and must lie at corners $(1, 1)$, $(c, 1)$, $(1, r)$, and (c, r). Each pair of neighboring points on the same horizontal or vertical line must be connected with an edge (or, line segment) and two different edges can intersect only at a control point. In $\vec{\mathbf{s}}$ and $\vec{\mathbf{t}}$, end condition knots may have multiplicity 4; all other knots are multiplicity $\leqslant 3$.

The equation of a T-spline surface is

$$\mathbf{T}(s,t) = \frac{\sum_{i=1}^{n_T} \mathbf{T}_i w_i T_i(s,t)}{\sum_{i=1}^{n_T} w_i T_i(s,t)} \tag{1}$$

or, in homogeneous form,

$$\mathcal{T}(s,t) = \sum_{i=1}^{n_T} (w_i \mathbf{T}_i, w_i) T_i(s,t) = \sum_{i=1}^{n_T} \mathcal{T}_i T_i(s,t) \tag{2}$$

where $\mathbf{T}_i = (x_i, y_i, z_i) \in \mathbb{R}^3$ are control points, $\mathcal{T}_i = (w_i x_i, w_i y_i, w_i z_i, w_i) \in \mathbb{P}^3$ are homogeneous control points, $w_i \in \mathbb{R}$ are weights, and n_T is the number of control points. The $T_i(s,t)$ in (1) and (2) are blending functions, with

$$T_i(s,t) = B[\vec{\mathbf{s}}_i](s) B[\vec{\mathbf{t}}_i](t) \tag{3}$$

where

$$\vec{\mathbf{s}}_i = [s_{\sigma_i^0}, s_{\sigma_i^1}, s_{\sigma_i^2}, s_{\sigma_i^3}, s_{\sigma_i^4}] \quad \text{and} \quad \vec{\mathbf{t}}_i = [t_{\tau_i^0}, t_{\tau_i^1}, t_{\tau_i^2}, t_{\tau_i^3}, t_{\tau_i^4}] \tag{4}$$

are subsequences of $\vec{\mathbf{s}}$ and $\vec{\mathbf{t}}$ respectively. $B[\vec{\mathbf{s}}_i](s)$ and $B[\vec{\mathbf{t}}_i](t)$ are cubic B-spline basis functions. Using the shorthand $\hat{s}_j = s - s_{\sigma_i^j}$ and $\hat{s}_{j,k} = s_{\sigma_i^j} - s_{\sigma_i^k}$,

$$B[\vec{\mathbf{s}}_i](s) = \begin{cases} 0, & s \leqslant s_{\sigma_i^0} \\ \frac{(\hat{s}_0)^3}{\hat{s}_{3,0}\hat{s}_{2,0}\hat{s}_{1,0}}, & s_{\sigma_i^0} < s \leqslant s_{\sigma_i^1} \\ \frac{-(\hat{s}_0)^2\hat{s}_2}{\hat{s}_{3,0}\hat{s}_{2,0}\hat{s}_{2,1}} + \frac{-\hat{s}_3\hat{s}_1\hat{s}_0}{\hat{s}_{2,1}\hat{s}_{3,1}\hat{s}_{3,0}} + \frac{-\hat{s}_4(\hat{s}_1)^2}{\hat{s}_{4,1}\hat{s}_{3,1}\hat{s}_{2,1}}, & s_{\sigma_i^1} < s \leqslant s_{\sigma_i^2} \\ \frac{\hat{s}_0(\hat{s}_3)^2}{\hat{s}_{3,0}\hat{s}_{3,1}\hat{s}_{3,2}} + \frac{\hat{s}_1\hat{s}_3\hat{s}_4}{\hat{s}_{3,2}\hat{s}_{3,1}\hat{s}_{4,1}} + \frac{(\hat{s}_4)^2\hat{s}_2}{\hat{s}_{4,1}\hat{s}_{4,2}\hat{s}_{3,2}}, & s_{\sigma_i^2} < s \leqslant s_{\sigma_i^3} \\ \frac{-(\hat{s}_4)^3}{\hat{s}_{4,1}\hat{s}_{4,2}\hat{s}_{4,3}}, & s_{\sigma_i^3} < s \leqslant s_{\sigma_i^4} \\ 0, & s_{\sigma_i^4} < s. \end{cases} \tag{5}$$

The values of $\vec{\mathbf{s}}_i$ and $\vec{\mathbf{t}}_i$ are determined as follows. The index coordinates of $\mathbf{T}_i$ are (σ_i^2, τ_i^2). Define an sK-point to be any $(i,j) \in \mathbb{Z}^2$ in a knot index diagram for which (i,j) contains a control point or a vertical edge, or for which $i \notin [1,c]$. Then σ_i^1 is the largest integer $< \sigma_i^2$ for which (σ_i^1, k) is an sK-point, σ_i^0 is the largest integer $< \sigma_i^1$ for which (σ_i^0, k) is an sK-point, σ_i^3 is the smallest integer $> \sigma_i^2$ for which (σ_i^3, k) is an sK-point, and σ_i^4 is the smallest integer $> \sigma_i^3$ for which (σ_i^4, k) is an sK-point. Likewise, a tK-point is any $(i,j) \in \mathbb{Z}^2$ for which (i,j) contains a control point or a horizontal edge, or for which $j \notin [1,r]$, and τ_i^1 is the largest integer $< \tau_i^2$ for which (τ_i^1, k) is a tK-point, etc. For the T-mesh in Fig. 1(a), $\vec{\mathbf{s}}_5 = [s_4, s_8, s_{10}, s_{11}, s_{12}]$, $\vec{\mathbf{t}}_5 = [t_{-1}, t_0, t_1, t_2, t_4]$, $\vec{\mathbf{s}}_9 = [s_1, s_4, s_6, s_8, s_{10}]$, and $\vec{\mathbf{t}}_9 = [t_0, t_1, t_3, t_5, t_6]$.

3. T-spline to NURBS conversion

The global knot vectors $\vec{\mathbf{s}}$ and $\vec{\mathbf{t}}$ can be used in defining a NURBS surface:

$$\mathbf{N}(s,t) = \frac{\sum_{j=1}^{c}\sum_{k=1}^{r} w_{jk}\mathbf{N}_{jk}N_{jk}(s,t)}{\sum_{j=1}^{c}\sum_{k=1}^{r} w_{jk}N_{jk}(s,t)} \tag{6}$$

where $\mathbf{N}_{jk}$ are control points, N_{jk} are basis functions, w_{jk} are weights, and r and c are the number of rows and columns in the control grid. In homogeneous form,

$$\mathcal{N}(s,t) = \sum_{j=1}^{c}\sum_{k=1}^{r} \mathcal{N}_{jk}N_{jk}(s,t) \tag{7}$$

where $\mathcal{N}_{jk}$ is the four-tuple $(w_{jk}\mathbf{N}_{jk}, w_{jk})$.

$$N_{jk}(s,t) = B_j(s)B_k(t) \tag{8}$$

where $B_j(s)$ and $B_k(t)$ are shorthand for

$$\begin{aligned} B_j(s) &= B[s_{j-2}, s_{j-1}, s_j, s_{j+1}, s_{j+2}](s), \\ B_k(t) &= B[t_{k-2}, t_{k-1}, t_k, t_{k+1}, t_{k+2}](t) \end{aligned} \tag{9}$$

as defined in (5), and the knots s_i and t_i belong to the global knot vectors. The index coordinates for N_{jk} are simply (j,k).

If $\mathcal{N}(s,t)$ and $\mathcal{T}(s,t)$ have the same global knot vectors, the $\mathcal{N}_{jk}$ can be uniquely determined such that $\mathcal{N}(s,t) \equiv \mathcal{T}(s,t)$, and the resulting $\mathcal{N}(s,t)$ is called the *underlying NURBS* of $\mathcal{T}(s,t)$. Fig. 1(b) shows the knot index diagram of the underlying NURBS for the T-mesh in Fig. 1(a).

Conversion from T-spline to underlying NURBS is best described using single subscript notation:

$$\mathcal{N}(s,t) = \sum_{l=1}^{n_P} \mathcal{N}_l N_l(s,t) \tag{10}$$

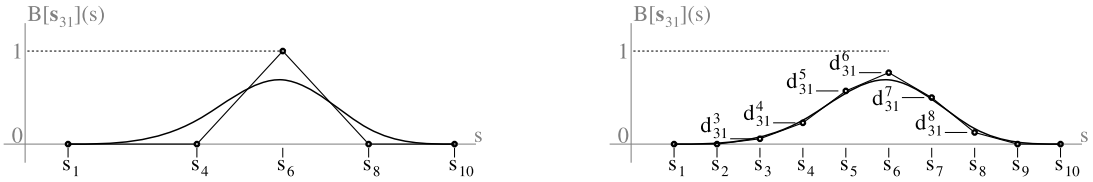

(a) Before refinement.

(b) After inserting knots at s_2, s_3, s_5, s_7, and s_9.

Fig. 2. Basis function $B[\vec{\mathbf{s}}_9](s)$ before and after refinement.

where n_P is the number of NURBS control points. Each double-subscript pair (j,k) in (7) can be mapped to a single subscript l in (10). For example,

$$l = \eta(j,k) = (k-1)c + j$$

defines a row-major ordering.

Each T-spline blending function can be written as a linear combination of NURBS basis functions:

$$T_i(s,t) = \sum_{j=1}^{n_P} m_{j,i} N_j(s,t) \tag{11}$$

where the $m_{j,i}$ are discussed in Section 3.1. Substituting (11) into (2),

$$\mathcal{T}(s,t) = \sum_{j=1}^{n_T} \mathcal{T}_j \left[\sum_{i=1}^{n_P} m_{i,j} N_i(s,t) \right] = \sum_{i=1}^{n_P} \left[\sum_{j=1}^{n_T} m_{i,j} \mathcal{T}_j \right] N_i(s,t) \tag{12}$$

which is equivalent to the NURBS surface (10) if

$$\mathcal{N}_i = \sum_{j=1}^{n_T} m_{i,j} \mathcal{T}_j. \tag{13}$$

This relationship can be written in matrix form:

$$M\mathbb{T} = \mathbb{P} \tag{14}$$

where $\mathbb{T} = [\mathcal{T}_1, \mathcal{T}_2, \ldots, \mathcal{T}_{n_T}]^T$ is a column vector of T-spline homogeneous control points $\mathcal{T}_i$ and $\mathbb{P} = [\mathcal{N}_1, \mathcal{N}_2, \ldots, \mathcal{N}_{n_P}]^T$ is a column vector of NURBS homogeneous control points $\mathcal{N}_i$, and M is an $n_P \times n_T$ matrix with elements $m_{j,i}$. We call M the *T-spline-to-NURBS transform matrix.*

M also expresses how the T-spline blending functions are linear combinations of NURBS basis functions. From (11),

$$\big(T_1(s,t), T_2(s,t), \ldots, T_{n_T}(s,t)\big) = \big(N_1(s,t), N_2(s,t), \ldots, N_{n_P}(s,t)\big) M. \tag{15}$$

3.1. Computing the elements of M

The $m_{j,i}$ elements of M are found by performing knot insertion into the T-spline blending functions (3). This is accomplished by inserting into $B[\vec{\mathbf{s}}_i](s)$ all knots that are in $\vec{\mathbf{s}}$ but not in $\vec{\mathbf{s}}_i$, and inserting into $B[\vec{\mathbf{t}}_i](t)$ all knots that are in $\vec{\mathbf{t}}$ but not in $\vec{\mathbf{t}}_i$. This yields

$$B[\vec{\mathbf{s}}_i](s) = \sum_{j=1}^{c} d_i^j B_j(s) \quad \text{and} \quad B[\vec{\mathbf{t}}_i](t) = \sum_{k=1}^{r} e_i^k B_k(t) \tag{16}$$

where the d_i^j and e_i^k result from knot insertion. We will illustrate using

$$T_9(s,t) = B[s_1, s_4, s_6, s_8, s_{10}](s) \cdot B[t_0, t_1, t_3, t_5, t_6](t)$$

from the example in Fig. 1(a). Into $B[\vec{\mathbf{s}}_9](s) = B[s_1, s_4, s_6, s_8, s_{10}](s)$ we insert s_2, s_3, s_5, s_7, and s_9 and into $B[\vec{\mathbf{t}}_9](t) = B[t_0, t_1, t_3, t_5, t_6](t)$ we insert t_2, and t_4. The result of insertion into $B[\vec{\mathbf{s}}_9](s)$ is illustrated in Fig. 2 where the blending functions are drawn as explicit B-spline curves.

Substituting (16) into (3),

$$T_i(s,t) = \sum_{j=1}^{c} \sum_{k=1}^{r} d_i^j e_i^k B_j(s) B_k(t). \tag{17}$$

Substituting (8) into (17) gives

$$T_i(s,t) = \sum_{j=1}^{c}\sum_{k=1}^{r} d_i^j e_i^k N_{jk}(s,t). \tag{18}$$

Comparing (18) with (11), we obtain the elements of M:

$$m_{\eta(j,k),i} = d_i^j e_i^k. \tag{19}$$

4. Determination of linear independence

The expressions $w_i T_i(s,t)/\sum_{j=1}^{n_T} w_j T_j(s,t)$ in (1) are called *rational* blending functions, and are determined by the T-mesh topology, knots, and weights. For a given topology, knots, and weights, the set of all rational blending functions form a linear space. If the rational blending functions are linearly independent, they form a basis of the space, whose dimension is n_T. For strictly positive weights w_i (assumed in practice), linear independence of the blending functions is equivalent to linear independence of the rational blending functions. Thus, the choice of (strictly positive) weights does not affect linear independence of the rational blending functions.

4.1. A necessary and sufficient condition for linear independence

Theorem 1. *The T-spline-to-NURBS transform matrix M for any T-spline surface is unique. Furthermore, a necessary and sufficient condition for a T-spline's blending functions to be linearly independent is that M is full rank.*

Proof. Referring to (15), since the $N_j(s,t)$ are B-spline *basis* functions, each column of M is unique, and so M itself is also unique.

By definition, T-spline blending functions are linearly independent if and only if there do not exist constants δ_i, not all zero, such that

$$\delta_1 T_1(s,t) + \cdots + \delta_{n_T} T_{n_T}(s,t) = (\delta_1, \ldots, \delta_{n_T}) \begin{pmatrix} T_1(s,t) \\ \vdots \\ T_{n_T}(s,t) \end{pmatrix} = 0.$$

From (15), this means that linear dependence requires

$$(\delta_1, \ldots, \delta_{n_T}) \begin{pmatrix} T_1(s,t) \\ \vdots \\ T_{n_T}(s,t) \end{pmatrix} = (\delta_1, \ldots, \delta_{n_T}) M^T \begin{pmatrix} N_1(s,t) \\ \vdots \\ N_{n_P}(s,t) \end{pmatrix} = 0.$$

Since $\{N_i(s,t)\}$ is a basis, the necessary and sufficient condition for linear dependence of the T-spline blending functions becomes

$$(\delta_1, \ldots, \delta_{n_T}) M^T = M \begin{pmatrix} \delta_1 \\ \vdots \\ \delta_{n_T} \end{pmatrix} = 0$$

for δ_i not all zero. But this will only happen if M is not full rank. □

Example. Fig. 3 shows a T-mesh that defines a set of linearly dependent blending functions, taken from (Buffa et al., 2010). The numbers on the left and on the bottom are knots. The matrix M in this case has a size of 56×40 and its rank is 39. As shown in Buffa et al. (2010), the blending functions T_1, T_2 and T_3 satisfy a linear relationship: $T_1(s,t) = T_2(s,t) + \frac{1}{3}T_3(s,t)$.

4.2. Column reduction

Recall that the dimension of the null space of a matrix is called its *nullity* and that for an $n_P \times n_T$ matrix M, $n_P \geqslant n_T$, the Rank-nullity theorem states that the nullity of M is $n_T - \text{rank}(M)$. Thus, linear independence of T-spline blending functions is equivalent to the nullity of M being zero.

If all elements of row j of M are zero except m_{ji}, column i is called an *innocuous* column. *Column reduction* is the operation of removing an innocuous column from M along with any zero rows that the column removal may have introduced. Denote by $\tilde{M}$ the matrix that results after performing all possible column reductions.

Lemma 2. *Nullity of an $n_P \times n_T$ matrix with $n_P \geqslant n_T$ is invariant under column reduction, so M and $\tilde{M}$ have the same nullity.*

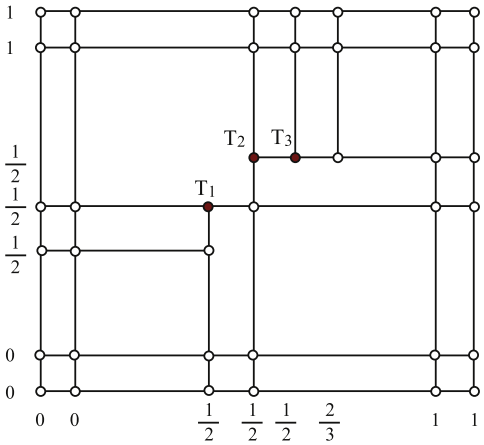

Fig. 3. A linearly dependent T-spline.

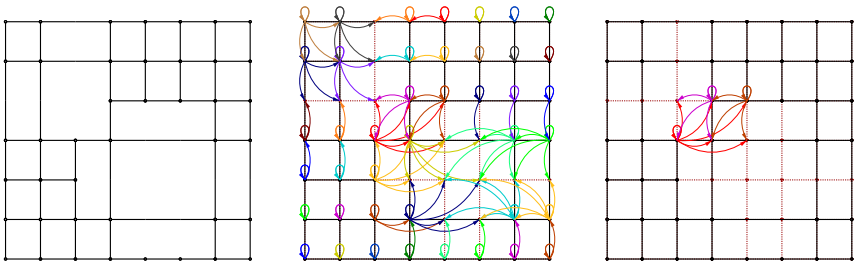

(a) T-mesh. (b) Influence graph G. (c) Fully pruned.

Fig. 4. A T-mesh and its influence graph.

Proof. Follows from the Rank-nullity theorem. □

Corollary 3. *If $\tilde{M} = \emptyset$, the T-spline's blending functions are linearly independent for all global knot vectors.*

$\tilde{M}$ is usually much smaller than M. For example, for the T-spline in Fig. 1(b), $\tilde{M} = \emptyset$. If $\tilde{M} \neq \emptyset$, $\tilde{M}$ can determine how knot choices influence the nullity of M. Consider the example in Fig. 3 and let $\vec{\mathbf{s}} = [s_0, s_1, s_2, s_3, s_4, s_5, s_6, s_7]$ and $\vec{\mathbf{t}} = [t_0, t_1, t_2, t_3, t_4, t_5, t_6]$. M is initially size 56×40. After column reduction, we obtain a 6×3 matrix:

$$\tilde{M} = \begin{bmatrix} \frac{t_4-t_1}{t_5-t_1} & \frac{(t_2-t_1)s_2}{(t_5-t_1)s_4} & 0 \\ \frac{(t_4-t_1)(s_6-s_4)}{(t_5-t_1)(s_6-s_1)} & \frac{(t_2-t_1)(s_5-s_2)}{(t_5-t_1)(s_5-s_1)} & \frac{(t_2-t_1)(s_2-s_1)}{(t_5-t_1)(s_5-s_1)} \\ \frac{(t_4-t_1)(s_6-s_4)(s_6-s_5)}{(t_5-t_1)(s_6-s_1)(s_6-s_2)} & 0 & \frac{t_2-t_1}{t_5-t_1} \\ \frac{t_6-t_4}{t_6-t_2} & \frac{s_2}{s_4} & 0 \\ \frac{(t_6-t_4)(s_6-s_4)}{(t_6-t_2)(s_6-s_1)} & \frac{s_5-s_2}{s_5-s_1} & \frac{s_2-s_1}{s_5-s_1} \\ \frac{(t_6-t_4)(s_6-s_4)(s_6-s_5)}{(t_6-t_2)(s_6-s_1)(s_6-s_2)} & 0 & 1 \end{bmatrix}.$$

A necessary and sufficient condition for $\tilde{M}$ to have non-zero nullity is for all of its 3×3 minors to vanish, which happens if and only if $s_2 = s_3 = s_4$ and $t_2 = t_3 = t_4$; the blending functions of this T-spline are linearly independent for any other choice of knots.

5. Influence graph

We can visualize column reduction using a directed graph G, drawn on a knot index diagram, that we call an *influence graph*. G contains two types of nodes: *T-nodes* correspond to T-spline control points, and *N-nodes* correspond to underlying NURBS control points. Edges in G originate at T-nodes and terminate at N-nodes and represent the non-zero elements of M: If m_{ij} is non-zero, an edge is drawn from T-node j to N-node i. A T-node and N-node that have the same index coordinates are said to correspond to each other, and every T-node points to its corresponding N-node. Fig. 4(b) shows the influence graph G for the T-mesh in Fig. 4(a).

The *valence* of an N-node is the number of edges that point to it. The valence of a T-node is the number of edges originating from it. An *innocuous node* is any T-node that points to at least one N-node of valence one, and represents

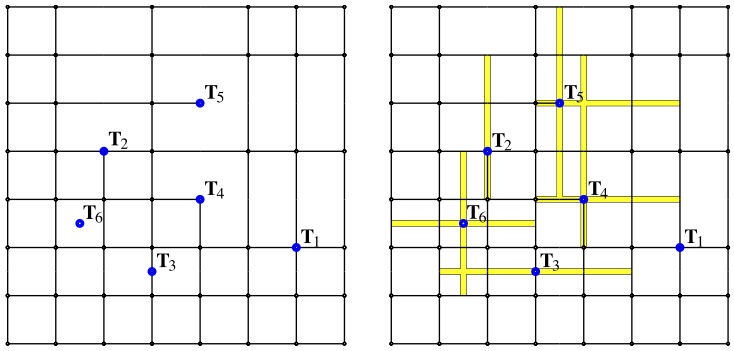

(a) T-mesh. (b) Extensions.

Fig. 5. T-mesh and extensions.

an innocuous column of M. *Pruning* a graph is the graphical equivalent of column reduction, and consists of eliminating an innocuous node, edges originating from it, and any N-nodes that no longer are pointed to. A graph from which all innocuous nodes have been pruned is said to be fully pruned. Fig. 4(c) shows the fully pruned version of Fig. 4(b).

A *subgraph* of G consists of any set of T-nodes, all N-nodes pointed to by those T-nodes, and all edges connecting those nodes. A *V2-subgraph* is a subgraph whose N-nodes all have a valence of at least two. A fully pruned graph is either empty, or consists of one or more V2-subgraphs. Fig. 4(c) shows a V2-subgraph with three T-nodes and six N-nodes.

Theorem 4. *If the influence graph for a T-mesh contains no V2-subgraphs, the T-spline has linearly independent blending functions.*

Proof. See Corollary 3, noting that pruning visualizes column reduction. □

$\mathbb{F}(\mathbf{T}_i)$ is the *footprint* of $\mathbf{T}_i$: the set of $\mathbf{N}_{jk}$ index coordinates pointed to by $\mathbf{T}_i$. Referring to (16), define $\mathbb{F}(\vec{\mathbf{s}}_i) = \{j \mid d_i^j \neq 0\}$, $\mathbb{F}(\vec{\mathbf{t}}_i) = \{j \mid e_i^j \neq 0\}$. Then, $\mathbb{F}(\mathbf{T}_i) = \mathbb{F}(\vec{\mathbf{s}}_i) \times \mathbb{F}(\vec{\mathbf{t}}_i)$ where "$\times$" is the Cartesian-product set operator.

Lemma 5. *Each N-node in a V2-subgraph $\tilde{G}$ is contained in the footprints of at least two T-nodes in $\tilde{G}$.*

Proof. Follows directly from the definition of a V2-subgraph. □

6. A topological condition for linear independence

This section presents a simple topological constraint that, when imposed on a T-mesh, assures linear independence of the T-spline's blending functions. Definition 6 calls any T-spline whose T-mesh satisfies this condition an analysis-suitable T-spline, for reasons outlined in the introduction. The constraint is expressed in terms of *T-node extensions*, which are line segments defined on a knot index diagram. Recall from Section 2 that the index coordinates of $\mathbf{T}_i$ are (σ_i^2, τ_i^2). If line segment $\overline{(\sigma_i^2, \tau_i^2)(\sigma_i^3, \tau_i^2)}$ is not an edge in the T-mesh, and $\sigma_i^3 \leqslant c$, then line segment $\overline{(\sigma_i^1, \tau_i^2)(\sigma_i^4, \tau_i^2)}$ is a T-node extension. Similarly, if $\overline{(\sigma_i^1, \tau_i^2)(\sigma_i^2, \tau_i^2)}$ is not a T-mesh edge, and $\sigma_i^1 \geqslant 1$, then $\overline{(\sigma_i^0, \tau_i^2)(\sigma_i^3, \tau_i^2)}$ is a T-node extension; if $\overline{(\sigma_i^2, \tau_i^1)(\sigma_i^2, \tau_i^2)}$ is not a T-mesh edge, and $\tau_i^1 \geqslant 1$, then $\overline{(\sigma_i^2, \tau_i^0)(\sigma_i^2, \tau_i^3)}$ is a T-node extension; and if $\overline{(\sigma_i^2, \tau_i^2)(\sigma_i^2, \tau_i^3)}$ is not a T-mesh edge, and $\tau_i^3 \leqslant r$, then $\overline{(\sigma_i^2, \tau_i^1)(\sigma_i^2, \tau_i^4)}$ is a T-node extension.

Fig. 5 shows T-nodes of various topological types and their extensions. A *T-junction* is a T-node that is connected to three edges and is not on the T-mesh boundary (such as $\mathbf{T}_2$) or a T-node that is connected to two parallel edges (such as $\mathbf{T}_3$). A T-node that is connected to only two perpendicular edges and is not on the T-mesh boundary (such as $\mathbf{T}_4$) is called an L-junction; T-nodes like $\mathbf{T}_5$ with one incident edge are called I-junctions, and T-nodes with no incident edges, like $\mathbf{T}_6$ are called isolated nodes. Since extensions are closed line segments, a horizontal and vertical extension can intersect either on the interior of both extensions (as in Fig. 6(a)) or at the endpoint of one or both extensions (as in Fig. 6(b)).

Definition 6. An analysis-suitable T-mesh is one for which no horizontal T-node extension intersects a vertical T-node extension. An analysis-suitable T-spline is one whose T-mesh is analysis-suitable.

L-junctions, I-junctions, and isolated nodes self-violate Definition 6 and thus are not allowed in an analysis-suitable T-mesh.

Theorem 7 is the main result of the paper.

Theorem 7. *Analysis-suitable T-spline surfaces have linearly independent blending functions.*

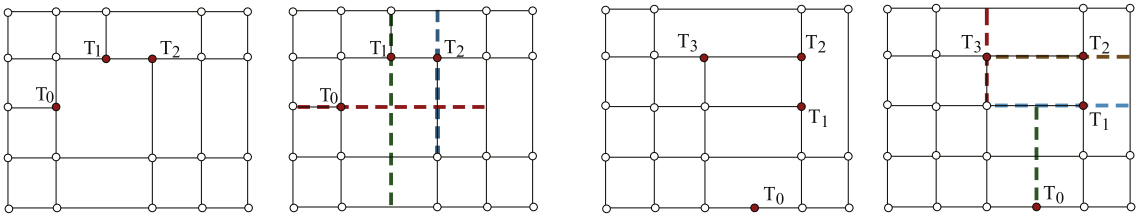

(a) Extensions that cross. (b) Extensions that touch.

Fig. 6. Extensions that intersect.

Proof. Given a T-mesh that has a V2-subgraph $\tilde{G}$, denote by $\mathbb{T}$ the set of T-nodes in $\tilde{G}$, and by $\mathbb{N}$ the set of index coordinates of N-nodes in $\tilde{G}$:

$$\mathbb{N} = \bigcup_{\mathbf{T}_i \in \mathbb{T}} \mathbb{F}(\mathbf{T}_i).$$

$\mathbb{N}$ contains at least one N-node (a, b) such that $\{(c, d) \in \mathbb{N} \mid c \leqslant a,\ d \leqslant b\} = \{(a, b)\}$. Denote one such point by $\mathbb{LL}$. Denote by $L(\vec{\mathbf{s}}_i)$ the smallest knot index in $\mathbb{F}(\vec{\mathbf{s}}_i)$, and let $LL_i = (L(\vec{\mathbf{s}}_i), L(\vec{\mathbf{t}}_i))$ denote the lower-left corner of $\mathbb{F}(\mathbf{T}_i)$. By Lemma 5, there must exist $\mathbf{T}_i, \mathbf{T}_j \in \mathbb{T}$ such that $LL_i = LL_j = \mathbb{LL}$, $\mathbf{T}_i \neq \mathbf{T}_j$.

$\mathbf{T}_i$ has index coordinates (σ_i^2, τ_i^2) and $\mathbf{T}_j$ has index coordinates (σ_j^2, τ_j^2). From Lemma 11, if $\sigma_i^2 = \sigma_j^2$ or $\tau_i^2 = \tau_j^2$, $LL_i \neq LL_j$. From Lemma 16, if $LL_i = LL_j$ and if $\sigma_i^2 > \sigma_j^2$ and $\tau_i^2 < \tau_j^2$ (or, if $\sigma_i^2 < \sigma_j^2$ and $\tau_i^2 > \tau_j^2$) there must be intersecting extensions, and from Lemma 17, if $LL_i = LL_j$ and if $\sigma_i^2 > \sigma_j^2$ and $\tau_i^2 > \tau_j^2$ (or, if $\sigma_i^2 < \sigma_j^2$ and $\tau_i^2 < \tau_j^2$) there must be intersecting extensions. Since analysis-suitable T-meshes have no intersecting extensions, Lemmas 11, 16, and 17 assure that they also have no V2-subgraphs and our proof follows from Theorem 4. □

6.1. Lemmas used in proving Theorem 7

This section presents Lemmas 11, 16, and 17 cited in Theorem 7.

Lemma 8.

(1) $L(\vec{\mathbf{s}}_i) = \sigma_i^0 + 2 \leqslant \sigma_i^1 + 1 \leqslant \sigma_i^2$ *if* $s_{\sigma_i^0} < s_{\sigma_i^0+1}$
(2) $L(\vec{\mathbf{s}}_i) = \sigma_i^0 + 2 = \sigma_i^1 + 1 \leqslant \sigma_i^2$ *if* $s_{\sigma_i^0} = s_{\sigma_i^0+1} < s_{\sigma_i^0+2}$; $\sigma_i^1 = \sigma_i^0 + 1$
(3) $L(\vec{\mathbf{s}}_i) = \sigma_i^0 + 2 = \sigma_i^1 + 1 \leqslant \sigma_i^2$ *if* $s_{\sigma_i^0} = s_{\sigma_i^0+1} = s_{\sigma_i^0+2}$; $\sigma_i^1 = \sigma_i^0 + 1$; $\sigma_i^2 = \sigma_i^0 + 2$
(4) $L(\vec{\mathbf{s}}_i) = \sigma_i^0 + 3 \leqslant \sigma_i^1 + 1 \leqslant \sigma_i^2$ *if* $s_{\sigma_i^0} = s_{\sigma_i^0+1} < s_{\sigma_i^0+2}$; $\sigma_i^1 \geqslant \sigma_i^0 + 2$
(5) $L(\vec{\mathbf{s}}_i) = \sigma_i^0 + 3 = \sigma_i^1 + 2 \leqslant \sigma_i^2$ *if* $s_{\sigma_i^0} = s_{\sigma_i^0+1} = s_{\sigma_i^0+2}$; $\sigma_i^1 = \sigma_i^0 + 1$; $\sigma_i^2 \geqslant \sigma_i^0 + 3$
(6) $L(\vec{\mathbf{s}}_i) = \sigma_i^0 + 3 = \sigma_i^1 + 1 \leqslant \sigma_i^2$ *if* $s_{\sigma_i^0} = s_{\sigma_i^0+1} = s_{\sigma_i^0+2}$; $\sigma_i^1 = \sigma_i^0 + 2$
(7) $L(\vec{\mathbf{s}}_i) = \sigma_i^0 + 4 = \sigma_i^1 + 1 \leqslant \sigma_i^2$ *if* $s_{\sigma_i^0} = s_{\sigma_i^0+1} = s_{\sigma_i^0+2}$; $\sigma_i^1 \geqslant \sigma_i^0 + 3$.

Proof. This can be verified by performing knot insertion into $B[\vec{\mathbf{s}}_i](s)$. □

Lemma 9. *If* $\vec{\mathbf{s}}_i, \vec{\mathbf{s}}_j \subset \vec{\mathbf{s}}$, $\sigma_i^1 \leqslant \sigma_j^0$ *and* $\sigma_i^2 \leqslant \sigma_j^1$, *then* $L(\vec{\mathbf{s}}_i) < L(\vec{\mathbf{s}}_j)$.

Proof. $\sigma_i^0 < \sigma_i^1 \leqslant \sigma_j^0 < \sigma_j^1$ and $\sigma_i^1 < \sigma_i^2 \leqslant \sigma_j^1 < \sigma_j^2$.

If $\vec{\mathbf{s}}_i$ is Case 1, 2, 3, 4, 6, or 7 in Lemma 8, $L(\vec{\mathbf{s}}_i) \leqslant \sigma_i^1 + 1 \leqslant \sigma_j^0 + 1 < \sigma_j^0 + 2 \leqslant L(\vec{\mathbf{s}}_j)$. If $\vec{\mathbf{s}}_i$ is Case 5, $L(\vec{\mathbf{s}}_i) = \sigma_i^0 + 3 \leqslant \sigma_i^2 \leqslant \sigma_j^1 < \sigma_j^1 + 1 \leqslant L(\vec{\mathbf{s}}_j)$. □

Corollary 10. *If T-nodes* T_i *and* T_j *have index coordinates* (c, τ) *and* (d, τ) *with* $c < d$, *then* $L(\vec{\mathbf{s}}_i) < L(\vec{\mathbf{s}}_j)$.

Proof. Since T_i and T_j are on the same horizontal knot line, their knot quintuples $\vec{\mathbf{s}}_i = [s_{\sigma_i^0}, s_{\sigma_i^1}, s_{\sigma_i^2}, s_{\sigma_i^3}, s_{\sigma_i^4}]$ and $\vec{\mathbf{s}}_j = [s_{\sigma_j^0}, s_{\sigma_j^1}, s_{\sigma_j^2}, s_{\sigma_j^3}, s_{\sigma_j^4}]$ satisfy the conditions of Lemma 9. □

Lemma 11. *Given* $\mathbf{T}_i$ *and* $\mathbf{T}_j$, *if* $\sigma_i^2 = \sigma_j^2$ *and* $\tau_i^2 \neq \tau_j^2$, *or if* $\tau_i^2 = \tau_j^2$ *and* $\sigma_i^2 \neq \sigma_j^2$, $LL_i \neq LL_j$.

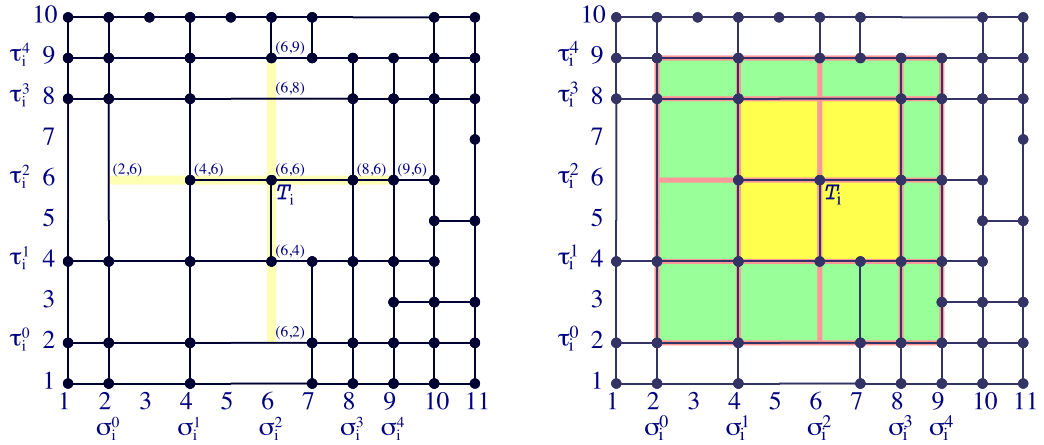

(a) K-nodes for $\mathbf{T}_i$. (b) One- and two-neighborhoods for $\mathbf{T}_i$.

Fig. 7. K-nodes and neighborhoods.

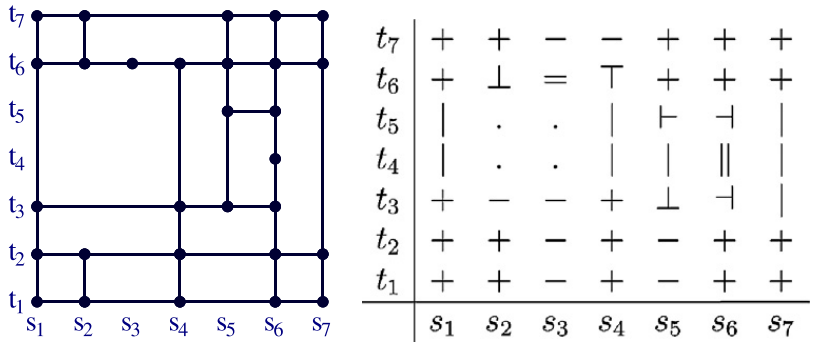

(a) T-mesh. (b) Symbol array.

Fig. 8. A T-mesh and its corresponding symbol array.

Proof. This follows directly from Corollary 10 and the definition of LL_i. □

Recall from Section 2 that the knot vectors in (4) for a T-node $\mathbf{T}_i$'s blending function were determined by five *s*K-points and five *t*K-points. We will refer to those nine points as $\mathbf{T}_i$'s K-points. In Fig. 7(a), $\mathbf{T}_i$'s K-points are labeled with index coordinates.

The K-points define a 4×4 grid of rectangles, $[\sigma_i^j, \sigma_i^{j+1}]\times[\tau_i^k, \tau_i^{k+1}]$, $j,k=0,1,2,3$, as illustrated in Fig. 7(b). The union of the four rectangular regions adjacent to $\mathbf{T}_i$, $[\sigma_i^1, \sigma_i^3]\times[\tau_i^1, \tau_i^3]$, is called the *one-neighborhood* of the domain of $\mathbf{T}_i$, and the union of the other 12 rectangles is called the *two-neighborhood* of the domain of $\mathbf{T}_i$. The bounding edges are considered part of the neighborhood. Thus, the boundary between the one- and two-neighborhoods lies in both neighborhoods.

Lemma 12. *If a T-mesh has no L-junctions, I-junctions, or isolated nodes, there is no T-node in the interior of the one-neighborhood of a T-node* **T***, other than* **T** *itself.*

Proof. Suppose there exists a T-node **P** in the interior of the one-neighborhood of the domain of a T-node T. **P** cannot be on one of the four edges incident to T because a T-node on the edges incident to T is a K-node. Thus **P** must be in the interior of the four rectangles adjacent to T. Without loss of generality, we assume that **P** lies in the interior of the north-east rectangle adjacent to T. Furthermore, we can assume **P** is the lowest T-node in this rectangle (if there are more than one T-node on that t-knot line, we choose the leftmost of them). Thus there is no edge connecting to **P** from below or from the left. Otherwise, the edge will hit the horizontal edge or the vertical edge incident to T and this will contradict the assumption that the rectangle is in the one-neighborhood of the domain of T. Thus **P** must be an L-junction, I-junction or isolated node, which violates the hypothesis. □

To discuss the topology of a T-mesh, we assign a symbol $\mathbb{S}_{ij}$ to each point in a knot index diagram $i\in[1,\ldots,c]$, $j\in[1,\ldots,r]$. The symbols describe topological elements of a T-mesh that has no L-junctions, I-junctions, or isolated nodes, as shown in Fig. 8. The possible symbols are:

$+$	Valence four T-node, corner T-node, or boundary T-node with three incident edges
$\vdash, \dashv, \perp, \top$	T-junction with three incident edges
$\|\|$	Vertical T-junction with two incident edges
$=$	Horizontal T-junction with two incident edges
$\|$	Vertical T-mesh edge
$-$	Horizontal T-mesh edge
$\cdot$	Does not correspond to a T-node or a T-mesh edge

For example, in Fig. 8, $\mathbb{S}_{2,6} = \perp$ and $\mathbb{S}_{6,4} = \|$. We will also use the notation $\mathbb{S}_{\mathbf{T}}$ or $\mathbb{S}_N$ to refer to the symbols at a labeled node $\mathbf{T}$ or N. For example, in Fig. 7(a), $\mathbb{S}_{\mathbf{T}_i} = \mathbb{S}_{6,6}$.

Lemma 13. *Allowable neighboring symbols for T-meshes that have no L-junctions, I-junctions, or isolated nodes are*:

$\mathbb{S}_{i,j}$	$\mathbb{S}_{i+1,j} \in$	$\mathbb{S}_{i,j+1} \in$	$\mathbb{S}_{i-1,j} \in$	$\mathbb{S}_{i,j-1} \in$
$+$	$\{+, \dashv, \perp, \top, =, -\}$	$\{+, \vdash, \dashv, \top, \|\|, \|\}$	$\{+, \vdash, \perp, \top, =, -\}$	$\{+, \vdash, \dashv, \perp, \|\|, \|\}$
$\vdash$	$\{+, \dashv, \perp, \top, =, -\}$	$\{+, \vdash, \dashv, \top, \|\|, \|\}$	$\{\|, \cdot\}$	$\{+, \vdash, \dashv, \perp, \|\|, \|\}$
$\dashv$	$\{\|, \cdot\}$	$\{+, \vdash, \dashv, \top, \|\|, \|\}$	$\{+, \vdash, \perp, \top, =, -\}$	$\{+, \vdash, \dashv, \perp, \|\|, \|\}$
$\perp$	$\{+, \dashv, \perp, \top, =, -\}$	$\{+, \vdash, \dashv, \top, \|\|, \|\}$	$\{+, \vdash, \perp, \top, =, -\}$	$\{-, \cdot\}$
$\top$	$\{+, \dashv, \perp, \top, =, -\}$	$\{-, \cdot\}$	$\{+, \vdash, \perp, \top, =, -\}$	$\{+, \vdash, \dashv, \perp, \|\|, \|\}$
$\|\|$	$\{\|, \cdot\}$	$\{+, \vdash, \dashv, \top, \|\|, \|\}$	$\{\|, \cdot\}$	$\{+, \vdash, \dashv, \perp, \|\|, \|\}$
$=$	$\{+, \dashv, \perp, \top, =, -\}$	$\{-, \cdot\}$	$\{+, \vdash, \perp, \top, =, -\}$	$\{-, \cdot\}$
$\|$	$\{\vdash, \|\|, \|, \cdot\}$	$\{+, \vdash, \dashv, \top, \|\|, \|\}$	$\{\dashv, \|\|, \|, \cdot\}$	$\{+, \vdash, \dashv, \perp, \|\|, \|\}$
$-$	$\{+, \dashv, \perp, \top, =, -\}$	$\{\perp, =, -, \cdot\}$	$\{+, \vdash, \perp, \top, =, -\}$	$\{\top, =, -, \cdot\}$
$\cdot$	$\{\vdash, \|\|, \|, \cdot\}$	$\{\perp, =, -, \cdot\}$	$\{\dashv, \|\|, \|, \cdot\}$	$\{\top, =, -, \cdot\}$

Proof. These relationships can be verified by considering each pair of neighboring symbols and observing which pairs are topologically possible. □

The notation $[\mathbb{S}_{i,j}, \mathbb{S}_{k,j})$, $i < k$, denotes either the sequence of symbols $\mathbb{S}_{i,j}, \ldots, \mathbb{S}_{k-1,j}$, or the set of symbols $\{\mathbb{S}_{i,j}, \ldots, \mathbb{S}_{k-1,j}\}$. Likewise, $(\mathbb{S}_{i,j}, \mathbb{S}_{i,k})$, $j < k$, can mean either the sequence of symbols $\mathbb{S}_{i,j+1}, \ldots, \mathbb{S}_{i,k-1}$, or the set of symbols $\{\mathbb{S}_{i,j+1}, \ldots, \mathbb{S}_{i,k-1}\}$. The meanings will be clear from the context. For example, in Fig. 8(b), $[\mathbb{S}_{1,2}, \mathbb{S}_{7,2}]$ can mean either $+, +, -, +, -, +, +$, or $\{+, -\}$; and $(\mathbb{S}_{5,2}, \mathbb{S}_{5,6}]$ can mean either $\perp, |, \vdash, +$ or $\{\perp, |, \vdash, +\}$.

Corollary 14. *Lemmas* 12 *and* 13 *lead to the following topological constraints for a T-mesh that has no L-junctions, I-junctions, or isolated nodes.*

(a) *If* $\mathbb{S}_{a,b} \in \{\cdot, -, \top, =\}$ *and* $\mathbb{S}_{a,c}$ *is a T-node symbol,* $b < c$*, and there are no T-node symbols in* $(\mathbb{S}_{a,b}, \mathbb{S}_{a,c})$*, then* $\mathbb{S}_{a,c} \in \{=, \perp\}$.
(b) *If* $\mathbb{S}_{a,c} \in \{\cdot, |, \dashv, \|\}$ *and* $\mathbb{S}_{b,c}$ *is a T-node symbol,* $b > a$*, and there are no T-node symbols in* $(\mathbb{S}_{a,c}, \mathbb{S}_{b,c})$*, then* $\mathbb{S}_{b,c} \in \{\vdash, \|\}$.
(c) *If* $\mathbb{S}_{a,b} \in \{\cdot, -\}$ *and* $\mathbb{S}_{a,c}$ *is an sK-node symbol,* $c > b$*, there is at least one T-node symbol in* $(\mathbb{S}_{a,b}, \mathbb{S}_{a,c}]$*. For the T-node with the smallest* $d \in (b, c]$*,* $\mathbb{S}_{a,d} \in \{=, \perp\}$.
(d) *If* $\mathbb{S}_{a,c} \in \{\cdot, |\}$ *and* $\mathbb{S}_{b,c}$ *is a tK-node symbol,* $b > a$*, there is at least one T-node symbol in* $(\mathbb{S}_{a,c}, \mathbb{S}_{b,c}]$*. For the T-node with the smallest* $d \in (a, b]$*,* $\mathbb{S}_{d,c} \in \{\|, \vdash\}$.
(e) *If* $\mathbb{S}_{a,c}$ *is a tK-node symbol and* $\mathbb{S}_{b,c} \in \{\cdot, |\}$*,* $b > a$*, there is at least one T-node symbol in* $[\mathbb{S}_{a,c}, \mathbb{S}_{b,c})$*. For the T-node with the largest* $d \in [a, b)$*,* $\mathbb{S}_{d,c} \in \{\|, \dashv\}$.
(f) *If there are no T-node symbols in* $(\mathbb{S}_{a,b}, \mathbb{S}_{a,c})$ *and* $\mathbb{S}_{a,c} \in \{\cdot, -\}$*,* $c > b$*, then* $\mathbb{S}_{a,b} \in \{\cdot, -, =, \top\}$.
(g) *If* $\mathbb{S}_{a,b}$ *is an sK-node symbol, and* $\mathbb{S}_{a,c} \in \{\cdot, -, =, \top\}$*,* $c > b$*, there is at least one T-node symbol in* $[\mathbb{S}_{a,b}, \mathbb{S}_{a,c}]$*. For the T-node with the largest value of* d*,* $b \leqslant d \leqslant c$*,* $\mathbb{S}_{a,d} \in \{=, \top\}$.
(h) *If a T-node with index coordinates* (b, e) *has a one-neighborhood rectangle with corners* (a, d) *and* (c, f) *with* $a < b < c$ *and* $d < e < f$*, then* $(\mathbb{S}_{a,d}, \mathbb{S}_{b,d}), (\mathbb{S}_{b,d}, \mathbb{S}_{c,d}) \subset \{\cdot, -, =, \top\}$*;* $(\mathbb{S}_{a,d}, \mathbb{S}_{a,e}), (\mathbb{S}_{a,e}, \mathbb{S}_{a,f}) \subset \{\cdot, |, \|, \dashv\}$*;* $(\mathbb{S}_{a,f}, \mathbb{S}_{b,f}), (\mathbb{S}_{b,f}, \mathbb{S}_{c,f}) \subset \{\cdot, -, =, \perp\}$*;* $(\mathbb{S}_{c,d}, \mathbb{S}_{c,e}), (\mathbb{S}_{c,e}, \mathbb{S}_{c,f}) \subset \{\cdot, |, \|, \vdash\}$.
(i) *If a T-node with index coordinates* (b, e) *has a one-neighborhood rectangle with corners* (a, d) *and* (c, f) *with* $a < b < c$ *and* $d < e < f$*, then for* $a < \bar{a} < b < \bar{c} < c$ *and* $d < \bar{d} < e < \bar{f} < f$*,* $(\mathbb{S}_{\bar{a},\bar{d}}, \mathbb{S}_{b,\bar{d}}), (\mathbb{S}_{b,\bar{d}}, \mathbb{S}_{\bar{c},\bar{d}}), (\mathbb{S}_{\bar{a},\bar{f}}, \mathbb{S}_{b,\bar{f}}), (\mathbb{S}_{b,\bar{f}}, \mathbb{S}_{\bar{c},\bar{f}}) \subset \{\cdot\}$*;* $(\mathbb{S}_{\bar{a},\bar{d}}, \mathbb{S}_{\bar{a},e}), (\mathbb{S}_{\bar{a},e}, \mathbb{S}_{\bar{a},\bar{f}}), (\mathbb{S}_{\bar{c},\bar{d}}, \mathbb{S}_{\bar{c},e}), (\mathbb{S}_{\bar{c},e}, \mathbb{S}_{\bar{c},\bar{f}}) \subset \{\cdot\}$.

Proof. These can be confirmed by repeated application of Lemma 13. □

Lemma 15. *Given a rectangle* R *in index coordinate space, with corners* (a, b) *and* (c, d)*,* ($a < c$ *and* $b < d$) *that satisfies one of these two conditions*:

1. *Either* $(\mathbb{S}_{a,b}, \mathbb{S}_{c,b}) \subset \{\cdot, -\}$ *or* $(\mathbb{S}_{a,d}, \mathbb{S}_{c,d}) \subset \{\cdot, -\}$*, and either* $(\mathbb{S}_{c,b}, \mathbb{S}_{c,d}) \subset \{\cdot, |, \|, \dashv\}$ *or* $(\mathbb{S}_{a,b}, \mathbb{S}_{a,d}) \subset \{\cdot, |, \|, \vdash\}$,
2. *Either* $(\mathbb{S}_{c,b}, \mathbb{S}_{c,d}) \subset \{\cdot, |\}$ *or* $(\mathbb{S}_{a,b}, \mathbb{S}_{a,d}) \subset \{\cdot, |\}$*, and either* $(\mathbb{S}_{a,d}, \mathbb{S}_{c,d}) \subset \{-, \cdot, =, \top\}$ *or* $(\mathbb{S}_{a,b}, \mathbb{S}_{c,b}) \subset \{-, \cdot, =, \perp\}$,

if the interior of R *contains a T-node, the T-mesh has intersecting extensions.*

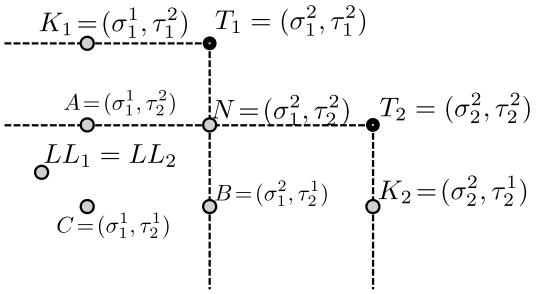

Fig. 9. K_1 and K_2 are K-nodes for T_1 and T_2, respectively.

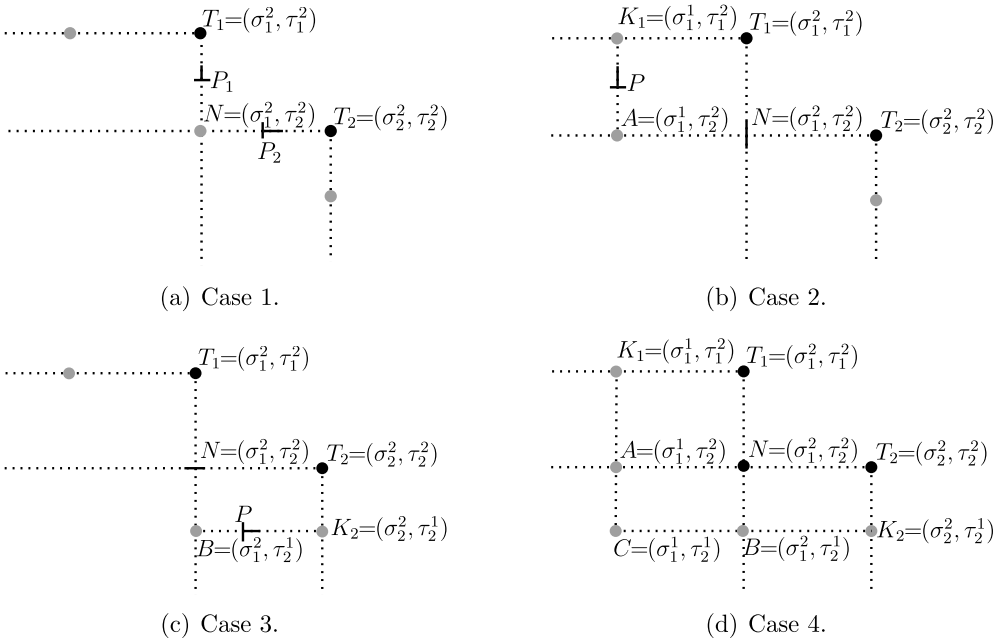

Fig. 10. Four different cases of Fig. 9.

Proof. L-junctions, I-junctions or isolated T-nodes have intersecting extensions, and are not discussed further. We use the conditions $(\mathbb{S}_{a,d},\mathbb{S}_{c,d})\subset\{\cdot,-\}$ and $(\mathbb{S}_{c,b},\mathbb{S}_{c,d})\subset\{\cdot,|,\|,\dashv\}$. The other conditions have similar proofs.

Denote by **T** the highest T-node in the interior of R (if there are more than one T-node on that t-knot line, choose the rightmost of them). The index coordinates of **T** are (i,j). Reasoning from Lemma 13, $\mathbb{S}_{i,j+1}\neq|$ because $\mathbb{S}_{i,d}\in\{\cdot,-\}$ and there are no T-node symbols in $(\mathbb{S}_{i,j},\mathbb{S}_{i,d})$. Thus, $\mathbb{S}_{i,j}\in\{=,\top\}$. Since **T** was chosen to assure that no T-node symbols are in $(\mathbb{S}_{i,j},\mathbb{S}_{c,j})$ and again reasoning from Lemma 13, $(\mathbb{S}_{i,j},\mathbb{S}_{c,j})=\{-\}$ and $\mathbb{S}_{c,j}=\dashv$. **T** and the T-junction at (c,j) have intersecting extensions. □

Lemma 16. *Given two T-nodes* $\mathbf{T}_1$ *and* $\mathbf{T}_2$*, if* $\sigma_1^2<\sigma_2^2$ *and* $\tau_1^2>\tau_2^2$ *and if* $LL_1=LL_2$*, there must be intersecting extensions.*

Proof. L-junctions, I-junctions, or isolated nodes have self-intersecting extensions, so are not considered further. Referring to Fig. 9, we analyze the four possible cases for the symbol at N and show that extensions intersect in each case.

Case 1. N is type "$\cdot$" (see Fig. 10(a)). Denote by P_1 the lowest T-node between N and T_1 inclusive. From Corollary 14(a), P_1 must be of type "$\perp$" or "$=$". Denote by P_2 the leftmost T-node between N and T_2 inclusive. From Corollary 14(b), P_2 is of type "$\vdash$" or "$\|$". By Lemma 9, $\tau_1^0<\tau_2^2$ and $\sigma_2^0<\sigma_1^2$ if $LL_1=LL_2$. Thus the extensions of P_1 and P_2 intersect at N.

Case 2. N is type "$|$" (Fig. 10(b)). N a K-node of T_2. There can be no T-node or node of type "$|$" between N and T_2, else LL_2 would lie to the right of N while LL_1 would not. By Lemma 9, if A is a K-node of T_2, $LL_1\neq LL_2$; therefore, $\mathbb{S}_A\in\{\cdot,-\}$. From Corollary 14(b), T_2 must be a T-junction of type "$\vdash$" or "$\|$". Since K_1 is a K-node of T_1, it must be a T-node or a node of type "$|$". $(\mathbb{S}_A,\mathbb{S}_{K_1}]$ contains at least one T-node symbol. Denote the lowest one by $\mathbb{S}_P$. From Corollary 14, $\mathbb{S}_P\in\{\perp,=\}$ and $(\mathbb{S}_A,\mathbb{S}_P)\subset\{\cdot\}$. The extensions of P and T_2 intersect at A.

Case 3. N is type "$-$" (see Fig. 10(c)). Since Cases 3 and 2 are symmetric, the extensions of P and T_1 intersect at B.

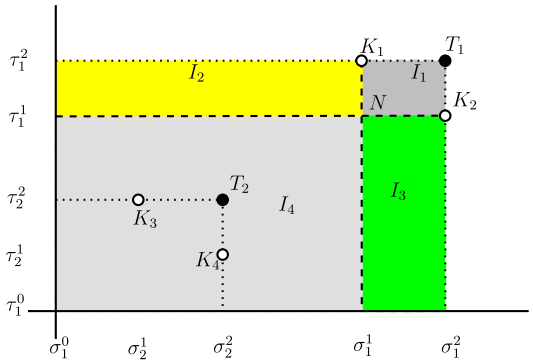

Fig. 11. K_1 and K_2 are K-nodes for T-node T_1. K_3 and K_4 are K-nodes for T-node T_2. I_1 is a one-neighborhood rectangle of T_1 and I_2, I_3, I_4 are two-neighborhood rectangles.

Case 4. N is a T-node (see Fig. 10(d)), making N a K-node of T_1 and T_2. Then there is no T-node symbol or "|" in $[\mathbb{S}_A, \mathbb{S}_N) \cup (\mathbb{S}_N, \mathbb{S}_{T_2})$; otherwise $LL_2 \neq LL_1$ by Lemma 9. There is no T-node symbol or "−" in $[\mathbb{S}_B, \mathbb{S}_N) \cup (\mathbb{S}_N, \mathbb{S}_{T_1})$; otherwise $LL_1 \neq LL_2$. Since K_1 is a K-node of T_1, it must be a T-node or a node of type "|". By Corollaries 14(h) and 14(i), $\mathbb{S}_{K_1} \in \{\perp, =\}$ and $[\mathbb{S}_C, \mathbb{S}_A) \cup (\mathbb{S}_A, \mathbb{S}_{K_1}) \subset \{\cdot\}$. Similarly, we can show that $\mathbb{S}_{K_2} \in \{\vdash, \|\}$ and $[\mathbb{S}_C, \mathbb{S}_B) \cup (\mathbb{S}_B, \mathbb{S}_{K_2}) \subset \{\cdot\}$. Thus the extensions of K_1 and K_2 intersect at C. □

Lemma 17. *Given two T-nodes* $\mathbf{T}_1 = (\sigma_1^2, \tau_1^2)$ *and* $\mathbf{T}_2 = (\sigma_2^2, \tau_2^2)$*, if* $\sigma_1^2 > \sigma_2^2$ *and* $\tau_1^2 > \tau_2^2$ *and if* $LL_1 = LL_2$*, there must be intersecting extensions.*

Proof. L-junctions, I-junctions, and isolated nodes have self-intersecting extensions so are excluded from further discussion.

Referring to Fig. 11, let $\mathbb{I}(I_k)$ denote the interior of I_k. By Lemma 8, since $LL_1 = LL_2$, $\sigma_1^0 < \sigma_2^2$ and $\tau_1^0 < \tau_2^2$, so $\mathbf{T}_2 \in \mathbb{I}(I_1 \cup I_2 \cup I_3 \cup I_4)$. The six possible locations for $\mathbf{T}_2$ are:

$\mathbf{T}_2 \in \mathbb{I}(I_1)$. By Lemma 12, this is not possible.

$\mathbf{T}_2 \in \mathbb{I}(I_3)$. Since (σ_1^2, τ_1^0) and K_2 are K-nodes of $\mathbf{T}_1$, there are no other tK-nodes between them. Corollary 14(h) requires $(\mathbb{S}_N, \mathbb{S}_{K_2}) \subset \{\cdot, -, =, \top\}$, so by Lemma 15, if $\mathbf{T}_2 \in \mathbb{I}(I_3)$ there are intersecting extensions.

$\mathbf{T}_2 \in \mathbb{I}(I_2)$. By similar reasoning, this also requires intersecting extensions.

$\mathbf{T}_2 \in (\mathbb{S}_N, \mathbb{S}_{K_2})$. Since $LL_1 = LL_2$ Lemma 9 requires $\tau_2^1 > \tau_1^0$, so $K_4 \in \mathbb{I}(I_3)$. By Corollary 14(e), there is at least one T-node $\in \mathbb{I}(I_3)$. By Lemma 15, there are intersecting extensions.

$\mathbf{T}_2 \in (\mathbb{S}_N, \mathbb{S}_{K_1})$. By similar reasoning, this also creates intersecting extensions.

$\mathbf{T}_2 \in (\sigma_1^0, \sigma_1^1] \times (\tau_1^0, \tau_1^1]$. From Lemma 9, $LL_1 = LL_2$ requires $\sigma_1^0 < \sigma_2^1$. Therefore $\sigma_1^0 < \sigma_2^1 < \sigma_2^2 \leqslant \sigma_1^1$. Similarly, $\tau_1^0 < \tau_2^1 < \tau_2^2 \leqslant \tau_1^1$. We analyze four possible cases for the symbol at N.

Case 1: N is type "·" (Fig. 12(a)). Lemma 13 and Corollaries 14(c) and 14(h) assure K_1 is type "⊥" or "=", and $(\mathbb{S}_N, \mathbb{S}_{K_1}) \subset \{\cdot\}$. From Corollaries 14(d), 14(h) and Lemma 13, K_2 is of type "⊢" or "‖" and $(\mathbb{S}_N, \mathbb{S}_{K_2}) \subset \{\cdot\}$. The extensions of K_1 and K_2 intersect at N.

Case 2: N is type "|" (see Fig. 12(b)). From Corollaries 14(d), 14(h) and Lemma 13, K_2 is of type "⊢" or "‖" and $(\mathbb{S}_N, \mathbb{S}_{K_2}) \subset \{\cdot\}$.

By a similar analysis as we did earlier for I_3, the interior of I_2 contains no T-node, and thus from Corollary 14(f), $\mathbb{S}_Q \in \{\cdot, -, =, \top\}$. For sK-node K_3, from Corollary 14(g), there exists a T-node symbol on $[\mathbb{S}_{K_3}, \mathbb{S}_Q]$ and the highest such T-node (call it Q') is type "=" or "⊤". The extension of Q' intersects the extension of K_2, unless there is a T-node symbol in $(\mathbb{S}_Q, \mathbb{S}_N)$. But from Corollary 14(f), any T-node symbol in $(\mathbb{S}_Q, \mathbb{S}_N)$ is "⊤" or "=". The rightmost such T-node has an extension that intersects that of K_2.

Case 3: N is type "−" (see Fig. 12(c)). Since Cases 2 and 3 are symmetric, the proofs are also symmetric.

Case 4: N is a T-node. If N is not T_2, there must exist a T-node Q_1 between (σ_1^0, τ_1^1) and N; otherwise, I_4 satisfies the conditions of Lemma 15 which assures that the interior of I_4 contains no T-node. But the proof for Case 2 confirms that the interior of I_4 contains a T-node. Similarly, we can prove that there must exist a T-node Q_2 between (σ_1^1, τ_1^0) and N. Corollary 14(f) assures that Q_1 is of type "⊤" or "=". Similarly, Q_2 must be of type "‖" or "⊣". Choose Q_1 and Q_2 such that there are no T-node symbols in $(\mathbb{S}_{Q_1}, \mathbb{S}_N)$ and $(\mathbb{S}_{Q_2}, \mathbb{S}_N)$, as illustrated in Fig. 12(d). Corollary 14(h) assures that either the extensions of Q_1 and Q_2 cross at M, or else if there is a T-node symbol in $(\mathbb{S}_{Q_1}, \mathbb{S}_M)$, it represents a T-junction whose extension will cross with Q_1's extension, or else if there is a T-node symbol in $(\mathbb{S}_{Q_2}, \mathbb{S}_M)$, it represents a T-junction whose extension intersects that of Q_2.

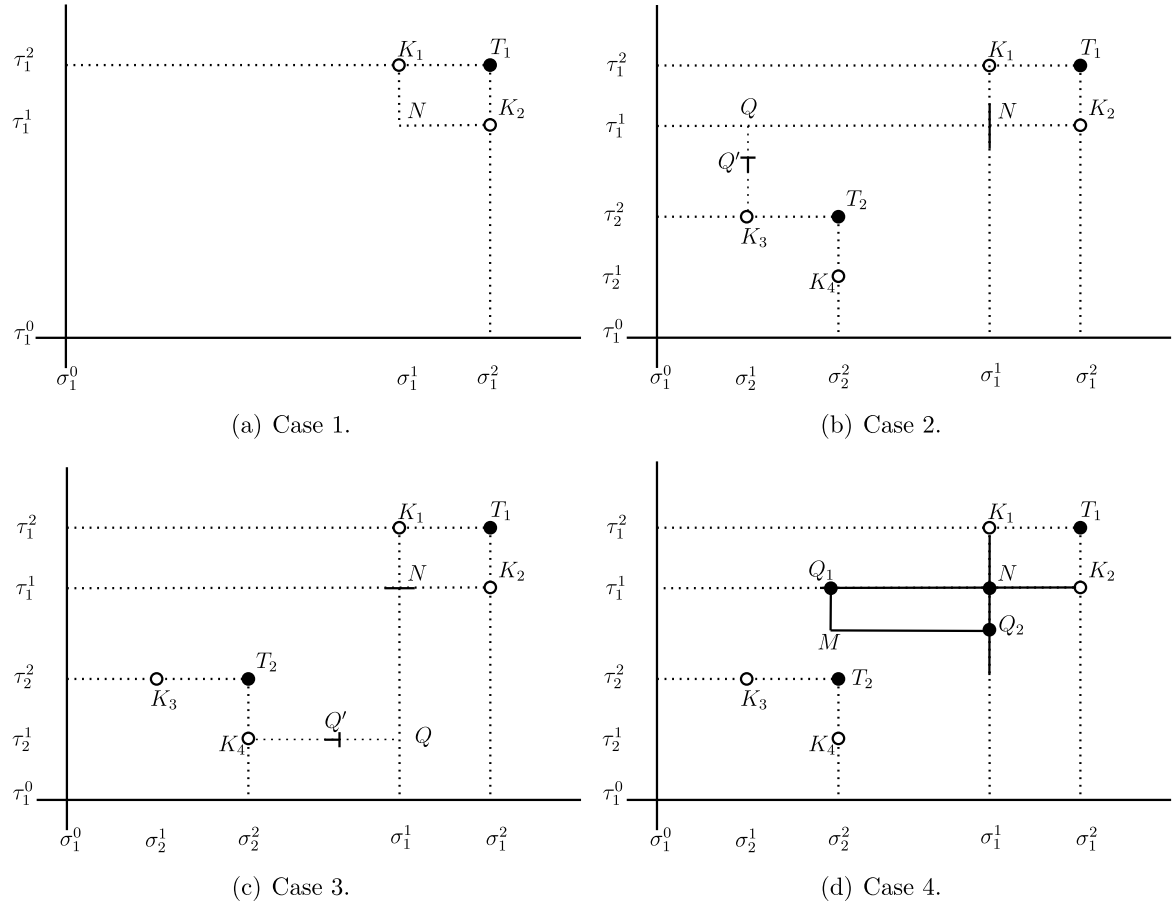

Fig. 12. Four different cases of Fig. 11.

If N is T_2, by Corollary 14(f), K_3 and K_4 are T-nodes and thus can serve as Q_1 and Q_2, and we can prove in the same way that there exist intersecting extensions. □

7. Conclusion

This paper presents algebraic and topological methods for analyzing linear independence of T-spline blending functions. We show that any T-spline whose T-mesh contains no V2-subgraphs has linearly independent blending functions for all choices of knots, and that analysis-suitable T-splines always have linearly independent blending functions because they contain no V2-subgraphs. Analysis-suitable T-splines thus provide a solid mathematical foundation for isogeometric analysis. Future papers will show that analysis-suitable T-splines can be locally refined (Scott et al., 2011) and provide a partition of unity (Li et al., 2011).

The results in this paper suggest several interesting problems for future research. The nullity of M can be expressed as a system of rational polynomial equations whose members are minors of the column-reduced M and whose variables are knots. What is the dimension of the solution set of such systems of equations? We conjecture that no T-mesh topology exists that has linearly dependent blending functions for all knots. Are there T-splines with linearly dependent blending functions that do not have multiple knots? How can the results of this paper be extended to T-meshes that have extraordinary points?

Acknowledgements

This work was supported by the Office of Naval Research ONR Grant Numbers N00014-08-C-0920 and N00014-08-1-0992, and by the ARC 9/09 Grant (MOE2008-T2-1-075) of Singapore. The first author was supported by grants from NSF of China (No. 11031007, No. 60903148), the Chinese Universities Scientific Fund, and SRF for ROCS SE and CAS Startup Scientific Research Foundation.

References

Bazilevs, Y., Calo, V.M., Cottrell, J.A., Evans, J.A., Hughes, T.J.R., Lipton, S., Scott, M.A., Sederberg, T.W., 2010. Isogeometric analysis using T-splines. Computer Methods in Applied Mechanics and Engineering 199, 229–263.

Buffa, A., Cho, D., Sangalli, G., 2010. Linear independence of the T-spline blending functions associated with some particular T-meshes. Computer Methods in Applied Mechanics and Engineering 199, 1437–1445.

Cottrell, J., Hughes, T.J.R., Bazilevs, Y., 2009. Isogeometric Analysis: Toward Integration of CAD and FEA. John Wiley & Sons, Ltd.
Finnigan, G.T., 2008. Arbitrary degree T-splines. Master's thesis. Brigham Young University, Department of Computer Science.
Hughes, T., Cottrell, J., Bazilevs, Y., 2005. Isogeometric analysis: Cad, finite elements, nurbs, exact geometry and mesh refinement. Computer Methods in Applied Mechanics and Engineering 194, 4135–4195.
Li, X., Zheng, J., Sederberg, T.W., 2011. On T-spline classification. In preparation.
Mourrain, B., 2010. On the dimension of spline spaces on planar T-subdivisions. Technical Report Inria-00533187. Inria.
Scott, M.A., Hughes, T.J.R., Li, X., Sederberg, T.W., 2011. Local refinement of analysis-suitable T-splines. Submitted for publication.
Sederberg, T.W., Cardon, D.L., Finnigan, G.T., North, N.S., Zheng, J., Lyche, T., 2004. T-spline simplification and local refinement. ACM Trans. Graph. 23, 276–283.
Sederberg, T.W., Finnigan, G.T., Li, X., Lin, H., Ipson, H., 2008. Watertight trimmed NURBS. ACM Trans. Graph. 27, 1–8.
Sederberg, T.W., Zheng, J., Bakenov, A., Nasri, A., 2003. T-Splines and T-NURCCs. ACM Trans. Graph. 22, 477–484.